Dynamics of Vesicles in shear and rotational flows: Modal Dynamics and Phase Diagram

Norman J. Zabusky[*], Enrico Segre[†], Julien Deschamps[‡], Vasiliy Kantsler[§] and Victor Steinberg[*1]

[*] *Physics of Complex Systems, Weizmann Institute of Science, Israel*
[†] *Physics Services, Weizmann Institute of Science, Israel*
[‡] *IRPHE, Aix-Marseille Université & CNRS, Marseille, France*
[§] *DAMTP, Cambridge University, UK*

Despite the recent upsurge of theoretical reduced models for vesicle shape dynamics, comparisons with experiments have not been accomplished. We review the implications of some of the recently proposed models for vesicle dynamics, especially the Tumbling-Trembling domain regions of the phase plane and show that they all fail to capture the essential behavior of real vesicles for excess areas, Δ, greater than 0.4. We emphasize new observations of shape harmonics and the role of thermal fluctuations.

I. INTRODUCTION

In the last years there has been an upsurge of interest in the dynamical response of micro-objects to low Reynolds number shear and elongation flows. A large number of researchers have dealt with vesicles, including the groups of Steinberg (experiments)[1–4], Gompper (simulations)[5–8], Lebedev (theory)[9,10] and Misbah (theory and simulations)[11–14]. Others have studied, along similar lines, their next-of kin, capsules, like Seifert, Finken and Kessler (theory and simulations)[15,16], Skotheim and Secomb (theory and simulations)[17] and Bagchi and Kalluri (simulations)[18]. A common theme is the behavior of the microscopic object at the verge of dynamic regime transition. The different investigators have discussed an extended phenomenology of intermediate and purportedly peculiar motion regimes, supporting their findings by the use of the one or the other model, or numerical experiment.

For the simulations, there are two modes of investigation: one is direct numerical simulation (DNS) in two[8,19–21] or three[7] dimensions, which requires computational sophistication; the other involves the derivation of reduced dynamical models, usually in a *perturbative* framework for *nearly-spherical* objects, $\Delta << 1$, which yields a number of coupled nonlinear ODEs. The excess area of the vesicle $\Delta = (A/r_0^2) - 4\pi$ is assumed $\ll 1$, where A is the vesicle surface area and r_0 its characteristic radius, obtained from the vesicle volume $V = (4\pi/3)r_0^3$. Most of the experimental data[1–4] for Tank Treading (TT) is in the range $0.05 < \Delta < 2$ and for Trembling (TR) (called also vacillating-breathing, VB[22], and swinging[23]) is within $0.45 < \Delta < 2$.

The system of ODEs is then studied as a dynamical system, either analytically or numerically, and its phase space properties are listed. Proposed systems of this sort have included two[9–11,13], three[24], and recently 14 nonlinear ODE[12]. A recent review was presented by Vlahovska, Podgorski, and Misbah [14] which refers to the latest work of Misbah and colleagues[12] and includes vesicle results. Three important and inter-related issues, often neglected by most of the theoretical and numerical work, are: a) the

effect of thermal fluctuations (because vesicles are small and the bending energy of the membrane is comparable to the thermal energy); b) the applicability of perturbative results, to the more readily obtained excess areas, $\Delta > 0.4$; and c) the role of odd modes of the contour shape.

Following the literature, we survey three possible regimes of motion, namely (TT), (TR) and tumbling (TU). We present here as our benchmark an expanded data set including recent experimental work[4], with more attention to the dynamics of mode interactions. Experiments of longer duration and higher resolution are ongoing and will allow us to refine this benchmark. We also present a new analysis of our earlier published TT data[1,2], demonstrating the success of the scaling with respect to the dimensionless parameter Λ (defined in eq. (2) below).

The layout of the paper is as follows: in section II we critically review the dynamical models for vesicle shapes proposed in literature, which suggest useful non-dimensional parameters and provide a basis for laws to scale the experimental data. In section III we present a new analysis of early and recently published data on vesicles and properties of the three dynamical regimes observed: in subsection III A we recall the experimental setup and the methodology used to analyze vesicle contours, and in the following III B, III C and III D we review experimental findings concerning vesicles in their regimes. In section IV we consider the broader problem of the phase diagram of all regimes of motion. Section V presents our conclusions.

II. DYNAMICAL MODELS FOR VESICLE INCLINATION ANGLE AND SHAPE EVOLUTION

A. Models without noise

Among the reduced dynamical models mentioned in the introduction, we refer in detail to three which are derived from first principles for a near spherical vesicle,

$\Delta \ll 1$. A perturbation expansion in powers of $\sqrt{\Delta}$ had already been given by Seifert [25] for Helfrich membrane, which is represented by a series of spherical harmonics (modes). If harmonics greater than two, thermal noise and nonlinear terms above the third order in a free energy expansion are neglected, one obtains a system of two coupled ODE's: namely the system of Lebedeev, Turitsin and Vergeles [9,10] (LTV), that of Danker et al. [11] (DBPVM), and its later variant [13] (KFM). We concentrate on these models because of their central role in the recent discussion about regime transitions, because they do not contain ad hoc fitted parameters (as the three equation system of Noguchi [24] does), and because they can be easily simulated.

The ODE's describe the vesicle in terms of two dynamical variables Θ and ψ, associated with the shape and tilt, respectively. To avoid confusion we preserve the notation of most of the original papers, despite that the tilt ψ will be the quantity to be compared to the experimental inclination angle θ, and not Θ. The different regimes of vesicle motion are sought among the attractors of the resulting dynamical system: for instance a fixed point with positive ψ is identified with tank treading (TT), a limit cycle spanning the whole range $[-\pi, \pi]$ for ψ is identified with tumbling (TU), and a limit cycle spanning just the part of the range for ψ is identified with trembling (TR). Non-dimensional parameter choices determine the phase portrait of the system, the structural stability of phase space trajectories, and other issues, which are of concern in this paper. Domains in the parameter space leading to the one or the other dynamical regime, and their boundary lines, are referred as to the phase diagram, discussed further in section IV.

The equations of DBPVM read

$$\tau \partial_t \psi = \frac{S}{2}\left[\frac{\cos 2\psi}{\cos \Theta}\left(1 + \sqrt{\Delta}\Lambda_2 \sin \Theta\right) - \Lambda\right]$$

$$\tau \partial_t \Theta = -S\left[\sin \Theta - \sqrt{\Delta}\Lambda_1\left(\cos 4\Theta + \cos 2\Theta\right) + \right.$$
$$\left. -\sqrt{\Delta}\Lambda_2 \cos 2\Theta\right]\sin 2\psi + \cos 3\Theta \qquad (1)$$

and involve the non-dimensional parameters:

$$S = \frac{14\pi \eta r_0^3}{3\sqrt{3}\kappa}\frac{s}{\Delta}, \quad \Lambda = \frac{(23\lambda + 32)}{8\sqrt{30\pi}}\frac{\omega}{s}\sqrt{\Delta}, \quad \tau = \frac{S\Lambda\sqrt{\Delta}}{2\omega},$$
$$(2)$$

$$\Lambda_1 = \frac{\sqrt{10}}{28\sqrt{\pi}}\left(\frac{49\lambda + 136}{23\lambda + 32}\right), \quad \Lambda_2 = \frac{10\sqrt{10}}{7\sqrt{\pi}}\left(\frac{\lambda - 2}{23\lambda + 32}\right),$$

where $\lambda = \eta_{in}/\eta_{out}$ is the viscosity contrast, s and ω are respectively the strain rate and the vorticity of the ambient flow, and κ is the vesicle membrane bending rigidity modulus. We note that while Λ depends on both Δ and λ, Λ_1 and Λ_2 depend on λ alone. In the original form [11] these parameters are expressed using the dimensionless shear rate χ (also called the capillary number, Ca), i.e.

$$\chi = Ca = \frac{\eta r_0^3 \dot{\gamma}}{\kappa}, \quad S = \frac{7\pi}{3\sqrt{3}}\frac{\chi}{\Delta}, \quad \Lambda = \frac{23\lambda + 32}{8\sqrt{30\pi}}\sqrt{\Delta}, \quad (3)$$

$$\tau = \frac{7\sqrt{\pi}(23\lambda + 32)}{72\sqrt{10}}\frac{\chi}{\dot{\gamma}}.$$

We remark that this form refers to a pure shear flow, for which $s = \omega = \dot{\gamma}/2$. The set of parameters $\{\chi, \lambda, S, \Lambda, \Delta\}$ is in fact redundant, at least in pure shear; we include here all the definitions for reference, as different sets are used in the original papers.

The DBPVM model differs from the LTV in that it introduced "higher-order" terms, with additional parameters Λ_1 and $\Lambda_2 \ll \Lambda_1$ which are multiplied by the small parameter $\sqrt{\Delta}$ in equations (1). Further work by the same group [13] employed a variant of this model (KFM), in which only Λ_1 is present. The simpler LTV model, in turn, can be obtained from DBPVM just by setting $\Lambda_1 = 0$, $\Lambda_2 = 0$.

A further zero-temperature, 14-ODE dynamical model was introduced by Farutin, Biben, and Misbah [12], including the second and fourth spherical harmonics and neglecting all others. This model purports to be most realistic, although its results also disagree with the experiments presented here. The merit of this model seems to be its good agreement with unpublished 3D numerical simulations. Unfortunately, no details about either the analytical or the computational model are given; odd modes are absent since they would not be excited on an initially ellipsoidal vesicle and the applied shear (both are described by j=2 modes), in contradiction to experimental observations [2-4]. As shown in section III C, this is not the case, especially in the TU and TR regimes. Also the recent direct numerical simulations with thermal noise [8] mentioned below in section II B show TR states that are greatly distorted and contain odd harmonics.

The model used by Noguchi and Gompper [7,23], which also results in a system of two ODE's, can also be quoted in this respect, though in part phenomenological. This model expresses the dynamics of the vesicle inclination angle θ and of a shape parameter (asphericity) α by means of terms which have partially a theoretical justification and are partially the result of numerical evaluations on ellipsoidal shells. The inclination angle θ and the asphericity α of the object are coupled, and ad-hoc fit of the free energy function dependent on α is employed.

To benchmark the different models, aside of results available in the literature, we compared the predictions about the range of Λ or λ for which the TR regime should be observed, at fixed values of Δ. We choose Λ or λ because all proposed models predict TR in a stripe of the respective parameter space, with a weaker dependence on the second parameter, which is S or χ. Table I presents a summary of values obtained by different models - some as reported by the respective papers, some reproduced by our numerical solutions of these models. We confirmed the results for DBPVM, KFM and LTV in a direct way, integrating the equations in MATLAB using the `ode45()` integrator. We produced phase trajectories for selected values of the control parameters, and noted the ranges of values of the parameters at which different regimes of motion occur. We did not attempt to repro-

Paper	model type	Δ	S	χ	Λ_{TR}	λ_{TR}
Farutin et al.[12]	14 ODE, $q = 2, 4$	0.43	98.42	10	$1.83 \div 2.6$	$8 \div 12$
Vlahovska et al.[14]	14 ODE, $q = 2, 4$	0.43	12	1.22	$2 \div 2.2$	$8.91 \div 9.94$
		1.0	12	1.22	$2.38 \div 2.9$	$8.91 \div 9.94$
Noguchi and	2 ODE,	0.44	12	1.24	$1.82 \div 1.95$	$7.86 \div 8.5$
Gompper[23,26]	phenomenological	0.91	36.9	8	$2.05 \div 2.2$	$5.86 \div 6.36$
		1.44	23.5	8	$2.25 \div 2.4$	$4.96 \div 5.37$
Danker et al.[11] (DBPVM)	2 ODE, $q = 2$ $\Lambda_1 \neq \Lambda_2 \neq 0$	0.43	98.42	10	$1.43 \div 1.56$	$5.97 \div 24.01$
Kaoui et al.[13] (KFM)	2 ODE, $q = 2$, $\Lambda_1 \neq 0, \Lambda_2 \equiv 0$	0.2	211.61	10	$1.42 \div 1.56$	$9.33 \div 10.39$
		0.43	98.42	10	$1.42 \div 1.57$	$5.92 \div 6.70$
		1.0	42.32	10	$1.42 \div 1.615$	$3.51 \div 4.08$
LTV[9]	2 ODE, $q = 2$ $\Lambda_1 \equiv \Lambda_2 \equiv 0$	0.43	98.42	10	$1.41 \div 1.5$	$5.87 \div 6.33$

Table I. Comparison of ranges of parameters Λ and λ where trembling is observed, according to different models. While we relied on information contained in the paper referenced for the first four cases, we numerically simulated the dynamical system for the three two-ODE models, DBPVM, KFM and LTV. q denotes the harmonic modes included in the dynamical model.

duce the results of the 14 equation system of Farutin, Biben, and Misbah[12] (as insufficient details are given), and we report here data extracted from their original paper. The data for the model by Noguchi and Gompper[23] was derived from their Fig. 4b, (equivalent to Fig. 2a of Noguchi[26]). Fig. 2a of Noguchi[26] is in fact a phase diagram for $V^* = 0.95, 0.9, 0.85$ (or $\Delta = 0.44, 0.91, 1.44$, $\Delta = 4\pi \left[(1/V^*)^{2/3} - 1 \right]$) which is compared with experimental data further below in Figure 18. We based our comparison wherever possible on the parameter values $\Delta = 0.43$ and $\chi = 10$, because these are recurring values in the papers we refer to. From Vlahovska, Podgorski, and Misbah[14], we extracted the range for Λ from their Fig. 6, where $S \leq 12$, corresponding to just $\chi = 1.22$. In all models the boundaries of TR motion are anyway seen to depend little on χ at large S.

We can draw several conclusions from this comparison. The first and main one is the disagreement in the number of independent non-dimensional parameters required by each model: *all, except LTV, require more than two*, in contrast with what is observed in the experiment. The second conclusion is more quantitative: none of the models really predicts the observed parameter range for trembling motion (section IV). If we look at Λ, in particular, the differences in the predictions between DBPVM, KFM at different Δ, and LTV at any Δ turn out to be negligible, but all three models predict a narrower range of Λ for TR than observed. Also, the model of Farutin, Biben, and Misbah[12] gives a prediction disagreeing with every other model as well with the experiment. Finally, we remark that the TR regime is inadequately described in these models adopting a framework of the second and fourth harmonics without thermal noise, as a "vacillating-breathing" mode. As was pointed in our previous work[3,4], thermal noise and third harmonics are crucial for understanding the dynamics of the TR state.

B. Simulations with noise

Messlinger et al.[8] present the results of two dimensional simulations of vesicles based on multi-particle collision dynamics, or MPC numerical algorithms. This is a discrete particle method akin to dissipative particle dynamics and implicitly includes fluctuations due to thermal motion. It has been developed by Gompper, Noguchi and colleagues and applied to simulation of vesicles in two and three dimensions. Moreover, Noguchi[26], in his comprehensive study of vesicles forced with oscillatory shear flows, also includes MPC simulations with constant shear. His Fig. 1 presents selected shapes during TT, TR, and TU.

It is remarkable that the simulation in 2D, with noise, of Messlinger et al.[8] captures the essence of what we observe experimentally. The vesicle shapes, Fig. 3 (and the supplementary animation) of their paper show a "swinging" or "trembling" motion which exhibits concave regions of negative curvature in the contour and clearly includes higher odd and even harmonics of the radial displacement. Such shapes are similar to those we show in Figures 1 and 12 below. Also the tumbling motion shown by Messlinger et al.[8] contains higher odd and even harmonics, but unfortunately no power spectra which could be compared with our experiments (section III C).

Messlinger et al.[8] also compare the MPC simulations with the two ODE model for the vesicle shape of Noguchi and Gompper, mentioned in section II A, which is studied with the addition of noise forcing terms to both equations. In Fig. 5, *ibidem*, the MPC results are compared to phase space trajectories of the 2-ODE model, with and without forcing (left column MPC, right column, 2-

ODE). Trajectories of the α vs. θ are plotted for various parameter values, and it is apparent that, in all cases but the first, swinging and tumbling occur *intermittently*, i.e., for a large parameter range the dynamics is strongly dependent on the noise forcing. This behavior has also been remarked in the experiments, and leads to ambiguous classification of our TU-TR transition. Unfortunately, a complete phase diagram, comparable with others, is not included - Fig. 2 of Messlinger *et al.*[8] has a sample of only four points.

Noguchi and Gompper also discuss in their earlier papers[7,23] the addition of stochastic forcing terms to their system of two ODEs, which are identical in form to those in Messlinger *et al.*[8]. However, in Noguchi and Gompper[7] the effect of forcing is assessed only with respect to TT, while all the phase diagrams shown in their other papers are obtained in absence of stochastic forcing.

III. EXPERIMENTAL ANALYSIS OF VESICLE DYNAMICS IN SHEAR AND GENERAL FLOWS

In the following, we review experimental findings about vesicles in either of the three dynamical regimes mentioned, with particular attention to scaling laws and unifying parameters suggested by the theories discussed in section II. We present a quantitative comparison of the old[1,2] and new[3,4] data on the inclination angles of vesicles in TT motion, which was obtained by two different approaches and analyzed differently in the two sets of papers, and comment on the issue of the transition boundary from TT to TU and TT to TR regimes as function of Δ and λ, in old and new sets of the data. Then we present a new spectral analysis of shapes, in particular for long time series in TR regimes. We also relate to the recurrent motion observed in TR and TU, and comment about the observed time periodicity.

A. Experimental techniques, analysis, and definition of regime transition lines

Fluorescent vesicles with prescribed viscosity contrast λ are prepared and followed when immersed in either planar ambient flow with controlled strain s and vorticity ω, or shear flow with controlled shear rate $\dot{\gamma} = 2s$ in plane Couette and channel flow configurations. Many different vesicles are imaged in isolation, each for several values of either s, ω in plane linear flow, or of $\dot{\gamma}$ in shear flow. The experiments have been described previously, and we refer to our papers[1–4] for all details of the procedure. We remind that vesicles with $1 \leq \lambda \leq 9.19$ were studied in a shear flow[1–3], while only vesicles with $\lambda = 1$ were studied in general linear flow in Deschamps *et al.*[4]. The bending rigidity modulus of the vesicles was estimated to be $\kappa \simeq 25 k_B T$ in all the experiments.

Our experimental technique, described in Deschamps, Kantsler, and Steinberg[3], is capable of determining r_0 and Δ from the full reconstruction of the vesicle in three dimensions, but follows the vesicle motion only through the imaging of sectional cuts. Care is taken to maintain focus and obtain the largest (equatorial) section of the vesicle under examination. We maintain that the variations in contour shape observed are indicative of the dynamics taking part in three dimensions. In Figure 1 we show a representative example of an individual vesicle (defined by Δ and λ) that changes its regime of motion as the ambient general linear flow is changed by variation of ω/s.

We analyze the contours of the vesicle images, reconstructed at sub-pixel accuracy by an ad hoc fitting algorithm which locates the brighter edge of the vesicle. Such contours are then fitted by the ellipse possessing the same tensor of inertia of the vesicle sectional area, to define the major axis and the dominant orientation $-\pi/2 \leq \theta(t) \leq \pi/2$. Two different approaches to determine transition thresholds between TT and either TU or TR regimes were used in our earlier[1,2] and later[3,4] papers. In the latter[3,4], the regime of motion of the vesicle, at time extents during which flow parameters are kept constant, is classified automatically according to an empirical criterion:

- if $\sqrt{\left\langle (\theta(t) - \langle\theta\rangle)^2 \right\rangle} > \pi/5$, then the vesicle regime is tumbling (TU);

- if $\langle\theta\rangle > \sqrt{\left\langle (\theta(t) - \langle\theta\rangle)^2 \right\rangle}$, then the vesicle regime is tank treading (TT);

- otherwise, the regime is classified as trembling (TR).

in which $\langle\cdot\rangle$ denotes the time average. This criterion, based solely on the mean and rms fluctuation values of the inclination angle and somewhat arbitrary thresholds, proved itself simple and robust for isolated vesicles, well defined in shape. It works effectively in presence of noisy data, and avoids the need of phase-unwrapping the inclination angle to resolve TU.

The approach to the data undertaken in the early papers[1,2] is somewhat different, and needs to be elucidated before comparing the various data sets. The early experiments were conducted to investigate the TT dynamics, namely the dependence of the inclination angle θ on Δ and λ. In order to reduce the scatter in the data due to thermal noise, in particular at smaller values of λ, measurements were averaged over large ensembles of more than 500 vesicles of the same value of λ (see, for example, typical data in Fig. 2). At that time the value of λ could only be inferred from the preparation procedure, and the error on it was found from a representative measurement. In the later experiments, instead, vesicles were examined individually, and the error on λ, amount-
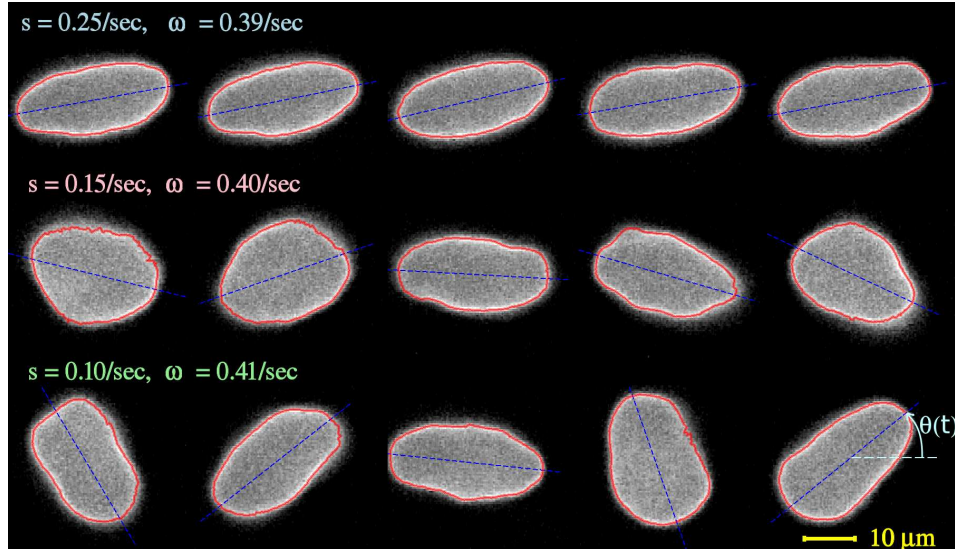
Figure 1. Imagery of a single vesicle with $\lambda = 1$ and $\Delta = 1.13$ driven into all regimes of motion. Snapshots are recorded every 1-2 sec. The red line (color online) is the reconstructed sectional contour, further analyzed for harmonics, and the blue dashed line is the major axis of the elliptical fit to the contour, according to whose motion the regime is classified automatically. The first row shows the vesicle in tank treading (note that the shape is almost elliptical, though random fluctuations are appreciable); the second row shows the vesicle during trembling (observe the remarkable changes of shape, with an occasional trilobed shape, indicative of a significant third harmonic). The last row shows the vesicle during tumbling. Here the definition of θ is presented.

ing to about 20%, could be estimated from direct measurements (see error estimates in Deschamps, Kantsler, and Steinberg[3]). Other parameters, like r_0 and Δ, were calculated from the cross-section measurements of each vesicle with an error of about 20% each, as well. Individually, χ depends cubically on r_0 (eq. (3)), and thus can vary strongly for different vesicles, even at the same shear rate in channel flow. The data ensemble was binned and averaged for some class values of Δ, and was presented as $\langle \theta(\Delta) \rangle$ for each λ available. For example, each curve in Fig. 1 of Kantsler and Steinberg[2] includes points resulting from many measurements on vesicles with different Δ and χ. At that time, from these ensemble averages, we concluded that θ does not depend on χ, in contrast to the recent theoretical findings of Kaoui, Farutin, and Misbah[13].

Figure 2. Inclination angle from ensemble of single vesicles in TT regime as a function of Λ for $\lambda = 1$ and $\eta = 10$mPa s. The straight line is is a linear fit to the data points.

B. Tank Treading: scaling of $\theta(\Lambda)$

A benchmark for the theories is the prediction of the vesicle inclination angle θ during TT, as function of the relevant control parameters. We have addressed the question in our early papers[1,2]. Very recently Farutin, Biben, and Misbah[12] have analyzed the problem using a part of our previously published data (from the figures in Kantsler and Steinberg[2]) and found it in good agreement with their model. Their presentation can be easily compared with that of a larger set of the data, in similar variables, shown by Vlahovska and Gracia[27]. Moreover, the plot in Farutin, Biben, and Misbah[12] suggests that
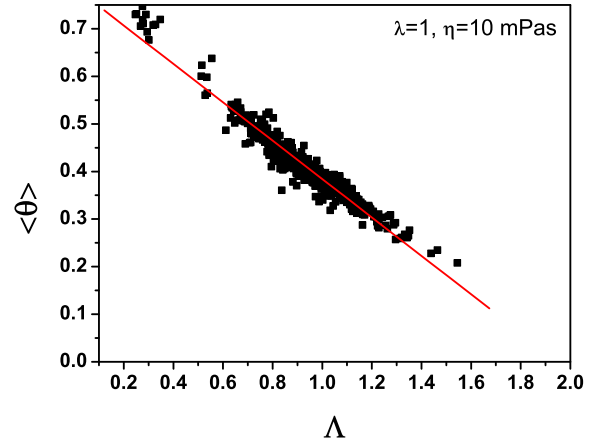
all data refers to $\chi=100$, while in Kantsler and Steinberg[2] the information about χ was not provided, for the reason just explained in section III A. To clarify the situation we rediscuss the old methodology and present more data supporting our view.

The data for θ can be plotted versus the one or the other representative quantity, like Δ or Λ; a functional dependence can be sought for single vesicles or for en-
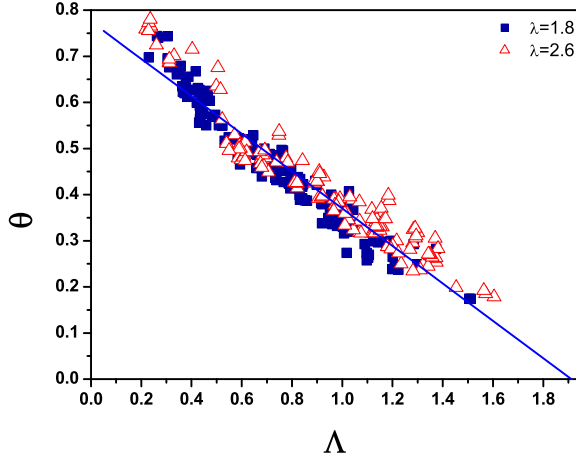
Figure 3. Inclination angle from an ensemble of individual vesicles in TT regime as a function of Λ, for two values of λ. The straight line is a linear fit to the data points.

Figure 4. Mean inclination angle obtained due to ensemble averaging in TT regime as a function of Δ for vesicles with different values λ presented on the plot (color online).

semble averages. In Fig. 2 and 3 we show $\theta(\Lambda)$ for single vesicles in the TT regime, respectively for $\lambda = 1$ and for $\lambda = 1.8, 2.6$. In spite of the scatter of the data due to thermal noise, the data collapse remarkably when plotted against the scaled variable Λ, and correlate well with a linear fit. The value Λ_c, defined by the intercept of the fit with $\theta = 0$, determines the transition, which is either to TU or to TR depending on S as discussed further. Compatible Λ_c are obtained in both plots, within the experimental error bars. The same was found for old data with $\lambda = 1$ and $\eta = 1.1$mPa s (not shown here). The supplementary material at [URL will be inserted by AIP] includes tabular data for $\lambda = 1.8$ and 2.6, with values of χ for each vesicle.

In Figure 4 we plot the data for $\langle \theta(\Delta) \rangle$ of vesicle ensembles. Part of this data were published in Kantsler and Steinberg[2], and are supplemented here by more values of λ. All available ensemble averaged data, at different λ, again collapse when plotted as function of the scaled variable Λ in Fig. 5 (analogously to what was done by Vlahovska and Gracia[27]). The dependence of $\langle \theta(\Delta) \rangle$ appears as a power law, except for tails at small θ and large Δ, seen for instance in Fig. 4, in particular for $\lambda = 3.4, 4.1, 4.9$ and 5.3. The tails are strikingly similar to those observed in the recent 2D numerical simulations of Messlinger $et\ al.$[8] (cfr. their Fig. 4) at comparable values of $\langle \theta \rangle \leq 0.15$ rad and $\Delta \geq 0.7$. Their tails are explained by the strong amplification of thermal fluctuations in the vicinity of the transitions to either TR or TU. The large scatter of the data at small θ and large Δ is responsible, in first instance, for deviations from the theoretical scaling in Fig. 2 of Vlahovska and Gracia[27]. The extrapolated value Λ_c corresponding to the intercept $\theta = 0$, marking the regime transition, cannot in fact be compared with a theory that ignores thermal noise.
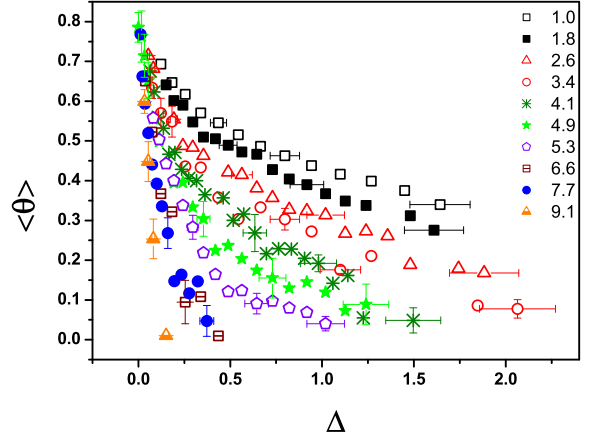
For these tails, the scaling exponent α in the dependence $\lambda_c \sim \Delta^\alpha$ (where λ_c is defined by extrapolation as with Λ_c), was found in Kantsler and Steinberg[2] to be about $-\frac{1}{4}$ rather than $-\frac{1}{2}$, as predicted later by the theory and found for the new data[3,4].

Excluding the data points related to the tails at small $\langle \theta \rangle$, large Δ and the values of λ mentioned above, the full set of Fig. 5 can be fitted within the error bars by $\langle \theta \rangle = 0.81 - 0.46\Lambda$. This fit provides $\Lambda_c = 1.74 \pm 0.2$. We emphasize that this data was obtained in shear flow at $\chi > 1$, which corresponds, according to eq. (3), to $S > S_c = \sqrt{3}$. In light of what became clear later on about the phase diagram for vesicles (see section IV), this means that the transition at these values of S is from TT to TR, and not to TU, as was suggested in Kantsler and Steinberg[2].

While there is experimental evidence for scaling of $\langle \theta(\Lambda) \rangle$, a theoretical regression law is more elusive. Theories by Seifert[25] for $\lambda = 1$, and Misbah[22] and Vlahovska and Gracia[27] for $\lambda \geq 1$, provide an exact solution for the inclination angle in TT up to its transition to TU, $\theta = \frac{1}{2}\cos^{-1}\Lambda$, giving $\Lambda_c = 1$. These theories do not account for a transition from TT to TR, whereas the LTV theory[9,10] discusses both possible transitions in detail. According to LTV, the transition TT-to-TU occurs for $S \leq \sqrt{3}$ at $\Lambda_c = 2/\sqrt{3} \approx 1.155$, while the transition TT-to-TR takes place at Λ_c up to $\sqrt{2} \approx 1.41$. The solution for the inclination angle in TT is found by solving the system (1) (with $\Lambda_1 = \Lambda_2 = 0$) with l.h.s. equal to zero. From the first of eq. (1), it can immediately be seen that this leads to $\theta = \frac{1}{2}\cos^{-1}[\Lambda\cos\Theta]$, where Θ can be represented in terms of S and Λ. After some algebra, a closed solution $\theta(\Lambda, S)$ is found, which is weakly dependent on S in the range $0 \leq \Lambda < 2/\sqrt{3}$, and bounded from above by its limit for $S = 0$, i.e. $\theta(\Lambda) = \frac{1}{2}\cos^{-1}\frac{\sqrt{3}\Lambda}{2}$. This

solution is displayed, for reference, for the specific values $S = 10$ and 50 in Figs. 5 and 6. The LTV solution is closer to the experimental data but still disagrees with it at $\Lambda \geq 0.8$ and $\langle \theta \rangle \leq 0.35$. Moreover the LTV theory predicts, for $S > \sqrt{3}$ and $2/\sqrt{3} < \Lambda < \sqrt{2 - 2/S^2}$, negative vesicle inclination angles, which we didn't observe, and a TT motion which is unstable in the third dimension and thus in practice not realized. Presenting part of the data of Fig. 5 binned in classes of Δ, rather than λ, we show clearly in Fig. 6 that either analytical solution matches satisfactorily the data only for $\langle \theta \rangle \geq 0.35$ and $\Delta \leq 1.42$. Better agreement between the LTV theory and the experiment is found only for the data in the lowest Δ bin, not surprisingly after the basic assumption of the theory, $\Delta \ll 1$. Thus, the extension of theoretical results beyond $\Delta \approx 0.15$ and small θ, used in particular in the recent publications[11–13], is unreasonable as it violates a basic assumption.

All experimental points corresponding to Δ=0.15, 0.24, and 0.42 at all values of $\langle \theta \rangle$ (except for two at $\Delta = 0.15$ and $\langle \theta \rangle$ close to zero) lie on the fitting straight line shown in Fig. 6, within the error bars. As for the comparison between the part of the data presented in Fig. 6 and the theory of Farutin, Biben, and Misbah[12], one cannot distinguish the theoretical curves corresponding to the lower Δ within the error bars. Only the data points shown by the open symbols, corresponding to $\Delta = 0.77$ and 1.42 and $\theta \leq 0.2$ and related to the enhanced thermal fluctuations at small θ and large Δ deviate from it. Thus, in our opinion, the quality of the experimental data does not allow one to distinguish between sets with different Δ within the error bars. Besides, as we demonstrated above, the full set of the data presented in Fig. 5 is also fitted rather well by a straight line in the whole range of $\langle \theta \rangle$ (once more, when the data points shown by open squares, related to the enhanced thermal fluctuations at small θ and large Δ at various λ are excluded). This conclusion brings us back to the problem, discussed in the recent theoretical[9–14] and experimental papers[3,4], whether a two or three-dimensional phase diagram is required to present all vesicle dynamical states. According to our statement, only two parameters are sufficient to account for the TT data within the error bars. If Farutin, Biben, and Misbah[12] were correct, the value of the transition Λ_c should depend on Δ, while we claim that for what can be understood from the available data, it is not. Further evidence for the regimes of TR and TU is discussed below in Section IV.

On the other hand, we found surprising and probably accidental that the linear approximation for $\Lambda \ll 1$ to the first solution, i.e. $\theta \approx \pi/4 - \Lambda/2$, describes the data rather well inside the error bars, and would give $\Lambda_c = \pi/2 \approx 1.57$. This was already pointed out in our early paper[1] and actually even used by Vlahovska and Gracia[27]. The linearization of the solution $\theta(\Lambda, S)$ of LTV would have a slightly milder slope and be as well compatible with the data, with Λ_c up to $\pi/\sqrt{3} \approx 1.81$.

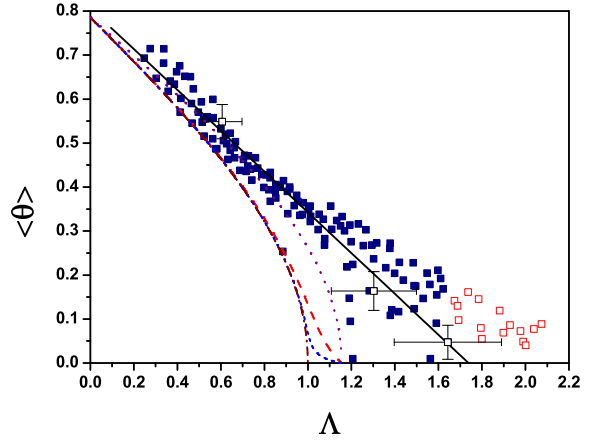The new data[3,4] were obtained differently. The de-

Figure 5. $\langle \theta(\Lambda) \rangle$ as a function of Λ, for the data in TT regime presented in Fig. 4, with some typical error bars. The full as well as the open squares present all the data with different λ and Δ; the open squares indicate the data at small θ and large Δ at various λ, susceptible to enhanced thermal fluctuations. The dash-dotted line (dark red online) is the theoretical solution $\theta = \frac{1}{2} \cos^{-1} \Lambda$; the other three reference lines are the LTV fixed point solution discussed in text, respectively for $S = 50$ (short dash, blue online), $S = 10$ (long dash, red online), and $S = 0$ (dot, purple online). The full straight line is a linear fit to the data, based on the full squares only, $\langle \theta \rangle = 0.81 - 0.46\Lambda$ with $\Lambda_c = 1.74$.
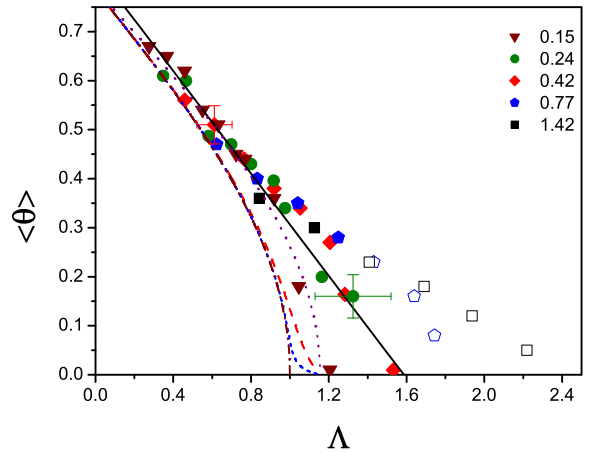

Figure 6. $\langle \theta(\Lambda) \rangle$ as a function of Λ for the TT data presented in Fig. 4, grouped in classes of Δ. The data points presented by open symbols corresponding to Δ =0.77 and 1.42 and $\theta \leq 0.2$ are related to the enhanced thermal fluctuations at small θ and large Δ. The full straight line is a linear fit to the data, based on the full symbols only, $\langle \theta \rangle = 0.83 - 0.52\Lambda$ with $\Lambda_c \simeq 1.6 \pm 0.2$. Reference dashed lines are the same as in Fig. 5 (color online).
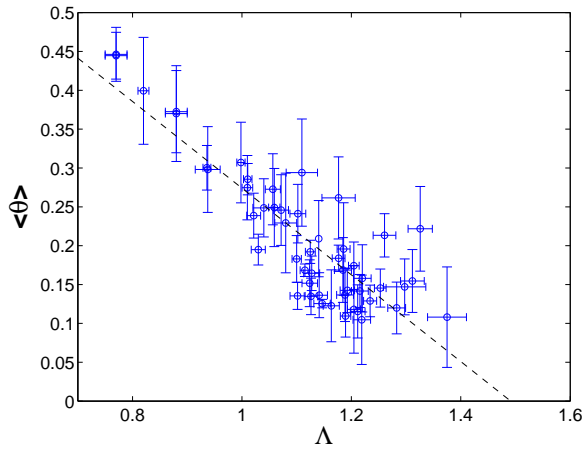
Figure 7. $\langle\theta\rangle$ versus Λ in TT regime for vesicles with $\lambda = 1$ in four-roll mill experiment. The dashed line is a linear fit to the data $\langle\theta\rangle = 0.83 - 0.56\Lambda$ with $\Lambda_c = 1.49$. Data points with $\langle\theta\rangle < 0.1$ and standard deviation larger than 0.07 are removed.

termination of the regime of motion of each vesicle as a function of Λ was conducted as explained in subsection III A. The experiments on vesicle dynamics were conducted in two different experimental devices and flow configurations. In the plane Couette flow apparatus only a minority of vesicles happened to be observed in the close vicinity of the transition, since λ and Δ, on which the parameter Λ depends, were not controlled but only measured[3]. Besides, a much smaller vesicle population was studied than in the old channel flow experiments; averaging on θ was done on short time series for single vesicles and not for ensembles. The resulting data is too sparse to analyze the TT motion and scaling, and, in spite of the smaller error bars and uncertainty in the determination of Λ and S, the transition lines on the phase diagram in e.g. Fig. 6 of Deschamps, Kantsler, and Steinberg[3] are marked by rather wide bands. In the four-roll mill device[4] instead, the control parameter ω/s was varied for each single vesicle with $\lambda = 1$ and measured Δ, and more data is available. In Fig. 7 we plot the data for $\langle\theta(t)\rangle$, averaged over the time versus Λ obtained in the four-roll mill device with the latter procedure, for vesicles in TT regime at $S > \sqrt{3}$. Again, data can be compared to theories only when the noisiest data, i.e. at small θ and large Δ, is excluded. The data that is fairly fitted by $\langle\theta\rangle = 0.83 - 0.56\Lambda$, giving $\Lambda_c = 1.49$, which is comparable to the value obtained for the old data (Fig. 5 and 6), to the approximate solutions, and even to the upper theoretical value $\Lambda_c = \sqrt{2}$ provided by LTV for unstable TT.

In summary, the collapse of all experimental data of $\langle\theta(\Lambda)\rangle$ supports only qualitatively the theoretical suggestion of the scaling[9,10,22,25,27]. This analysis also confirms that neglecting the thermal fluctuations leads to the scaling $\lambda_c \sim \Delta^{-1/2}$, which follows from $\Lambda_c = const$, for both the old and new experimental data.
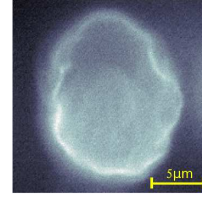

Figure 8. Image of a vesicle in TR, exhibiting multiple out-of-focus indentations suggesting a three-dimensional wrinkling-like perturbation. Quantitative analysis of the instantaneous three-dimensional shape is not possible with our technique.

C. Trembling: Analysis of experimental vesicle contours, dynamics of harmonics and thermal noise

TR, which is the intermediate state between TT and TU, turns out to be the key regime to understand the vesicle dynamics in a general linear flow. In this regime, the inclination angle θ oscillates around zero. During an oscillation cycle a given membrane patch periodically experiences both stretching and compression. Because of that, the TR dynamics is found to be more complex than even TU. The latter is also characterized by the periodic switching between stretching and compression, but the time spent under compression at small inclination angles in TR is much longer. This circumstance leads to stronger vesicle shape deformations in the TR regime due to the volume and surface area constraints and to extreme sensitivity to thermal noise at small θ. The occurrence of strong shape perturbations and the appearance of higher order harmonics resemble very much the wrinkling recently observed and studied in a time-periodic elongation flow[28,29]. In the latter case, the control parameter, which is the elongation rate, could be varied in order to find the onset of the instability and to study the nonlinear dynamics of higher order modes, above the onset. Here, like in TR, higher order modes (wrinkles) are generated during the compression period, due to the constraints. During compression, strong shape deformations present mostly as concavities of the vesicle, producing locally a negative surface tension, which in turn initiates the instability, with strong sensitivity to thermal noise. As the result, both even and odd higher order harmonics are generated. Their growth is arrested since compression acts for just a brief part of the period, but sometimes, at larger noise amplitude, vesicle budding occurs[28]. Similar effects of vesicle wrinkling and budding and pinching have been occasionally observed also in TR (see Figures 8, 9 and 10 and movies [URL will be inserted by AIP]). However, even the snapshots of a vesicle performing a more regular TR (e.g. Fig. 1) clearly demonstrate a drastic difference with the snapshots of the vacillating-breathing mode presented in Danker et al.[11]. In the VB mode the vesicle shape remains elliptical, within only even second and fourth harmonics and a vesicle indeed imitates breathing.
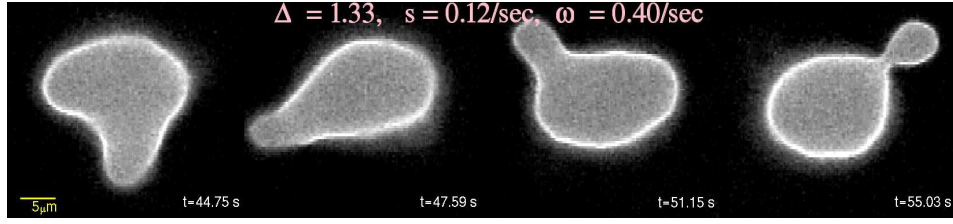
Figure 9. Vesicle with $\lambda = 1$, $\Lambda = 2.71$ and $S = 2.43$, generating a protrusion (pinching). The movie is available in the Supplementary Material [URL will be inserted by AIP].
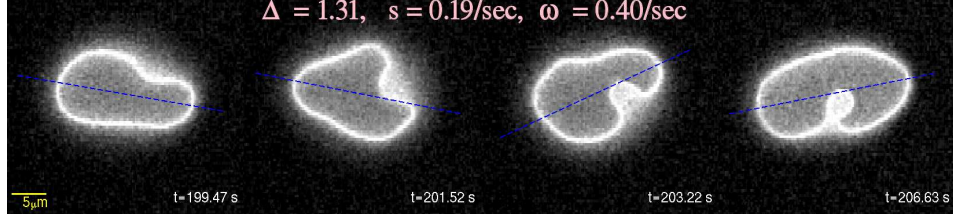

Figure 10. Trembling vesicle with $\lambda = 1$, $\Lambda = 1.72$ and $S = 9.75$, budding. The movie is available in the Supplementary Material [URL will be inserted by AIP].

To study quantitatively the TR dynamics, we analyzed the images of the experiments[3,4], looking at the radial amplitude of the contour $r(\phi, t)$, $0 \leq \phi \leq 2\pi$, relative to the centroid of the vesicle contour in each image. This radial profile is Fourier-decomposed, i.e. r is expressed as $r(\phi, t) = \sum_q \tilde{r}_q(t) e^{iq\phi}$. Observations about the interplay of different modes in time are presented in the following. We observe as a side remark, that even performing the Fourier decomposition in the frame of reference centered on the vesicle, there is no a priori geometrical symmetry guaranteeing that any particular contour harmonic is null or conserved. A translation of the frame of reference would alter all modes of the decomposition, but the fact that a particular mode (e.g. $q = 1$) is not null, is not at all an indication of a miscentered frame of reference.

Figure 11 displays the time evolution of the inclination angle $\theta(t)$ and of the amplitude of the lowest harmonic modes $A_q(t) = |\tilde{r}_q(t)|$ for a typical long trembling sequence, at constant s and ω. Trembling motion is seen to be characterized by recurrent, roughly periodic oscillations in the amplitude of the zero-th mode, accompanied by short duration dips in the amplitude of the second mode, correlated with peaks of the third. The latter means that the vesicle section periodically departs for a short time from its oval shape, to attain a more triangular appearance. This activity reflects fluctuations of the three-dimensional vesicle shape, since the fluctuations in the observed contour length corresponding to the perturbations in A_0 can occur only due to 3D effects, which are indeed observed in the experiment and resemble wrinkling (see Fig. 8). Some instantaneous contours of the vesicle during this sequence are shown in Figure 12 together with their spectra, notably around the time of one of such deformations. The intermediate power spectra in Fig. 12b clearly demonstrates the prevalence of the third mode over fourth and even second modes at the time when the vesicle contour (see Fig. 12a) is sort of triangular with an additional concavity. This is apparent in the movie provided as Supplementary Material [URL will be inserted by AIP]. From Figure 11 we also see that the time traces of the first few harmonics are correlated with modes 2 and 3, and that higher harmonics are decreasingly smaller and noisier as q increases. The inclination angle θ is seen to oscillate somewhat irregularly around zero, while the vesicle occasionally performs full tumblings. We observe this motion notably in flow conditions close to the TR/TU transition (see section IV below). Such irregularities led us to use the simple and robust regime classification criterion mentioned above.

Figure 13 provides an example of a vesicle driven into the three regimes, evidencing the evolution of the inclination angle and of the second and third contour modes. The second harmonic mode $A_2(t)$ peaks and dips irregularly during the TR oscillations, with a correlation of the dips with the minima of the inclination angle θ; during TU, this mode has minima in correspondence with $\theta \sim (2n + 1)\pi/2$, that is twice per full vesicle revolution. The increase in $A_3(t)$ passing from TT to TU and even more to TR is apparent, as well as the irregularity of TR motion.

Finally, in Figure 14(a) we show the spectra of the amplitudes $A_q = \langle A_q(t) \rangle$ of the harmonic modes of the contour averaged in time, for another vesicle with $\Delta = 0.64$, which was also driven in the three different regimes for some time. These spectra are typical of all cases observed, in the following sense: mode 1 is always small; modes 2 and 4 have mean amplitudes roughly independent from the regime; mode 3 and 5 are always a few times smaller in TT than in TR or TU. The amplitude A_3 is smaller for vesicles with smaller values of Δ. These
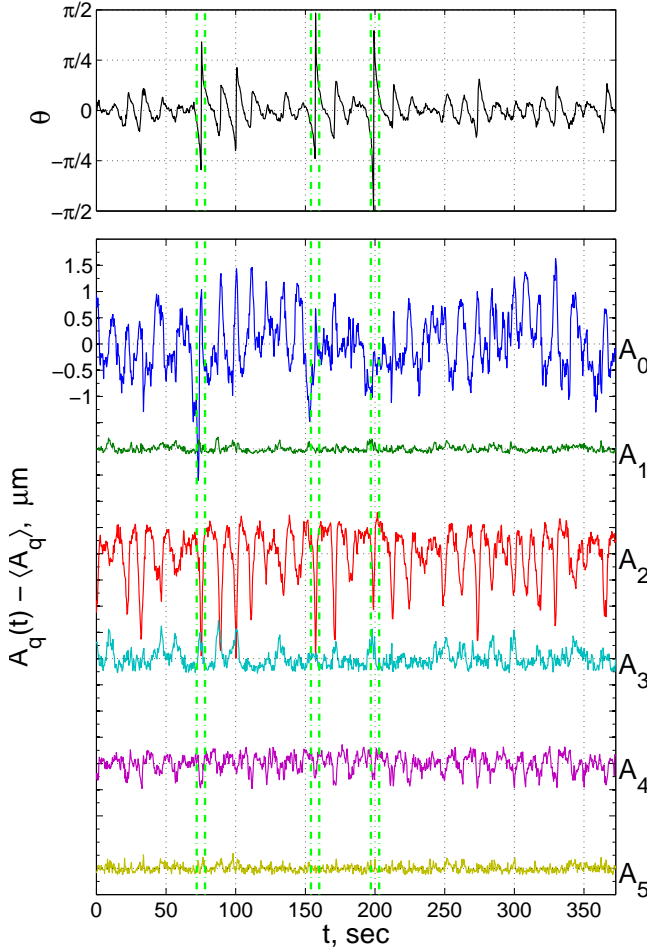
Figure 11. Upper panel: inclination angle $\theta(t)$ of of a vesicle with $\Delta = 1.16$ and $\lambda = 1$, during the course of a long trembling sequence. Lower panel: amplitudes $A_q(t)$ of the first harmonic modes of the sectional contour. For convenience of plotting, mean values have been subtracted, and time traces have been shifted vertically relative one to another $2\mu m$. Vertical dotted lines are added as a guide to the eye, to mark events of occasional *tumbling* (color online).

plots quantify the observation, seen by eye from images like those in Figure 1, that vesicles are "almost elliptical" during TT, while they undergo more elaborate shape changes during TR and TU. There seems in general to be no dependence, either on the regime or on Δ, of the decay spectrum of higher harmonics in the range $q \sim 6 \div 30$. For the same sequence, the mean squared fluctuations of the mode amplitudes, $a_q^2 = \langle (A_q(t) - \langle A_q \rangle)^2 \rangle$, are shown in Figure 14(b). It is interesting to note that the fluctuations of the lower order modes are much smaller in TT than in both TR and TU. The spectrum of fluctuations of a vesicle can be compared with the theoretical prediction of Seifert[30] in thermal equilibrium

$$a_q^2 = \epsilon(q, S) = \frac{r_0^2 k_B T}{\kappa(q-1)(q+2)[q(q+1) + \sigma r_0^2/\kappa]}, \quad (4)$$
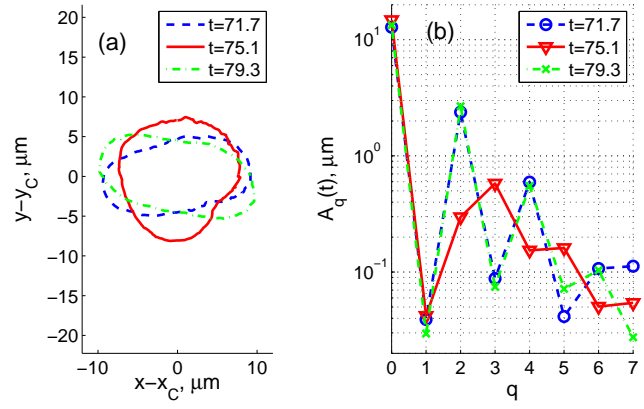

Figure 12. (a) Instantaneous contours in center-of-area coordinates, and (b) angular spectra of selected snapshots from the trembling sequence of figure 11. Note the significant decrease of A_2 and A_4 and the corresponding increase of A_3 for the intermediate contour (color online).

where σ is the surface tension. For large S the last term in the denominator can be expressed[25] as $\sigma r_0^2/\kappa = 0.77 S \sqrt{\Delta}$.

For large q, the expression (4) can be rewritten as

$$a_q^2 \simeq \frac{r_0^2 k_B T}{\sigma r_0^2 q^2 + \kappa q^4}. \quad (5)$$

It is remarkable in Figure 14(b) that the fluctuations for TR and TU are quite well described by this latter expression, with $\sigma \to 0$. An explanation of this fact may lie in the fact that the effective surface tension, which becomes locally negative during the compression of the membrane, averages out over an oscillation cycle of the vesicle.

D.   Regime transitions and oscillation periods of TR and TU

Figure 13, as well as the equivalent Fig. 5 of Deschamps, Kantsler, and Steinberg[3] and Fig. 4 of Deschamps *et al.*[4], also demonstrate the effect of a quick change of the control parameters, $\dot{\gamma}$ in the former and ω/s and s in the latter, on the vesicle motion. The time series of $\theta(t)$ shows an almost instantaneous change of the dynamical regime, within about a period, much shorter than the characteristic dynamical time τ. The theory[11] and the associated numerical simulations, without thermal noise, show instead very long transients, of duration of the order of χ^{-1}, which are not found in the experiments.

The characteristic oscillation period in either TR or TU is extracted from all available data like that presented in Figures 11 and 13. To this extent, we determined the dominant temporal frequency in $A_2(t)$ using the `pburg` function of `Matlab`; this frequency is divided by two in
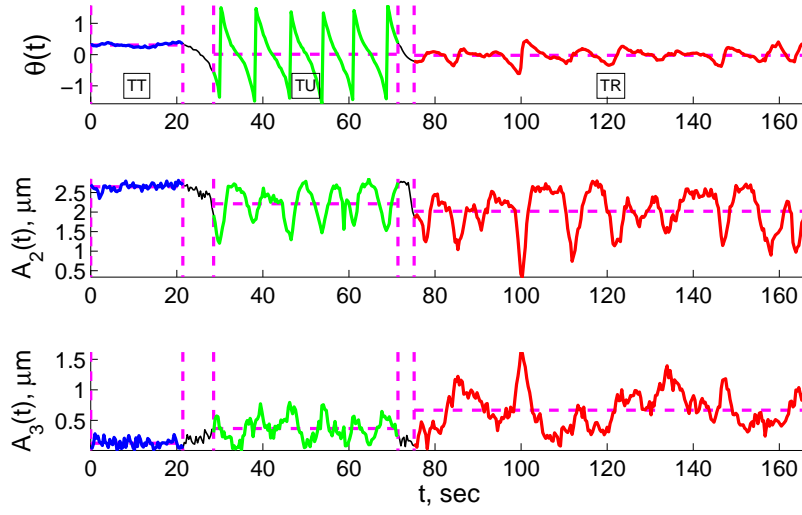
10

Figure 13. Instantaneous inclination angle $\theta(t)$ and amplitudes of the second and third angular harmonics $A_2(t)$ and $A_3(t)$ for a vesicle with $\Delta = 0.71$ and $\lambda = 1$ in a general flow, with s and ω kept constant for extended time and then quickly changed. Vertical (magenta online) dashed lines delimit stretches of constant flow, while horizontal dashed lines mark time averages. Note that the transition between one regime of motion and the next is sudden, and the transient appears to be shorter than one period (of either TR or TU) (color online).
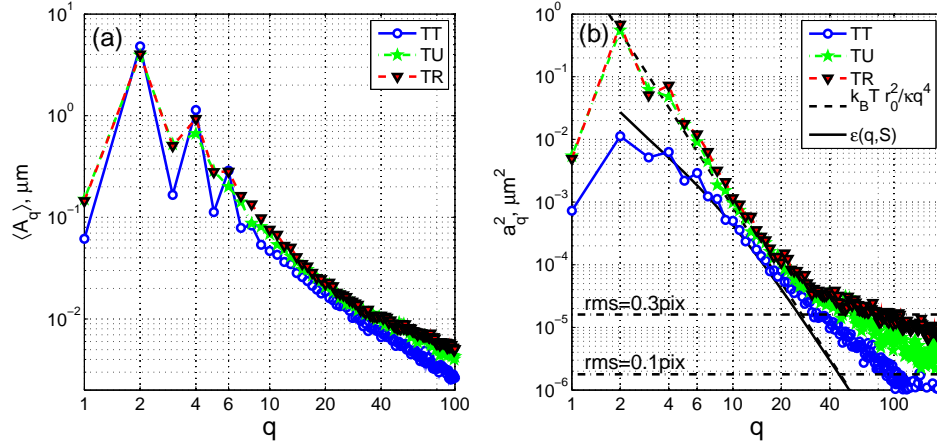

Figure 14. (a) Spectra of the mean contour harmonic modes $\langle A_q \rangle$ for a typical vesicle with $\Delta = 0.64$ and $\lambda = 1$, accessing the three regimes; (b) spectra of the squared fluctuations a_q^2 for the same sequence. The solid black line is the theoretical form $\epsilon(q, S)$ given in eq. (4), evaluated for $S = 114.11$, corresponding to the TT case. The dashed black line is the limiting form $\frac{k_B T r_0^2}{\kappa q^4}$. At high q, the spectra flatten due to the contour reconstruction noise. Horizontal dash-dotted lines corresponding to a white noise of amplitude 0.3 and 0.1 pixels are reported for reference, and demonstrate the subpixel accuracy of our analysis (color online).

TU, to account for the observed periodicity within one tumbling cycle. The resulting periods T, for the vesicle sequences of duration sufficient for a reliable estimate, are shown in Fig. 15, rescaled by either s or ω. Surprisingly, we didn't find any correlation between T and τ provided by eq. (2). We observed a large dispersion of periods in TR, while for large Λ the periods tend to $T \simeq 2\pi/\omega$ in TU regime, as expected for rigid body rotation. Correlation with Δ or χ, as predicted by theories (e.g. Kaoui, Farutin, and Misbah [13]) is not observed either.

Both the the fast regime adjustments and the observed

oscillation periods in TU and TR disprove, even qualitatively, the picture presented by the reduced theoretical models. Instead of a "breathing" of the vesicle shape in TR, observed in the models which employ the second and eventually the fourth order harmonics and without thermal fluctuations, we observe a noisy dynamics. The experimental picture found is one of strong mode interaction and correlation, with a pronounced role of the third harmonic, where thermal noise is considerably amplified. This underlying mechanism is very different from the viewpoint of the papers of Misbah's group [11–13,22], though
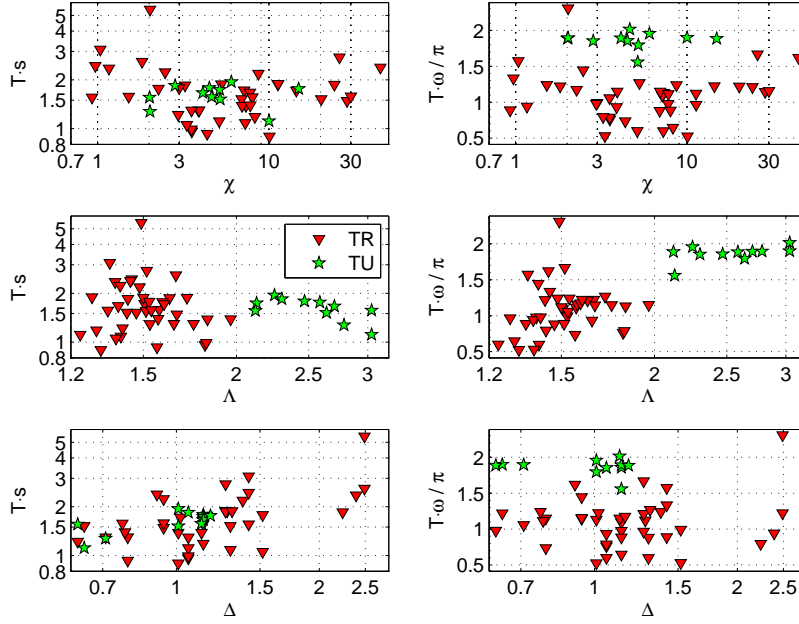
Figure 15. TR and TU periods, rescaled with s and ω (color online).

the vesicle shape deformations are comparable with those presented by Messlinger *et al.*[8]. For better appreciation the movie of TR dynamics provided in Supplementary Material [URL will be inserted by AIP] should be compared with the snapshots of the VB mode presented in Fig. 5 of Danker *et al.*[11].

IV. PHASE DIAGRAMS - COMPARISON WITH RECENT EXPERIMENTAL DATA

The study of the dynamical systems described in Section II leads to the construction of phase diagrams. That is, regions in the model parameters space, where the same regime of motion is attained. A similar approach has been applied to capsules[15–18]. While all authors agree on the existence of at least the three regimes of motion mentioned above, they dissent about the dimension of the phase space, and about the position of the regime boundaries in that space. According to LTV, the phase space is $\{S, \Lambda\} \in [0, \infty[\times [0, \infty[$; according to DBPVM and KFM the phase space is three dimensional, and better represented by the group $\{Ca, \lambda, \Delta\}$. The choice of LTV scaling has clearly the advantage of simplicity, and, as we want to demonstrate, probably accounts for the correct scaling in powers of $\sqrt{\Delta}$, though it agrees only qualitatively with the experiment. To assess this, we plot all available data in the one or the other parameter space, and compare the results.

Figure 16 shows our most recent phase diagram, which includes data for vesicles with $0.015 < \Delta < 2.5$ from the experiments[1–4] and extends the parameter ranges. Classification of regimes is automatic for the data of
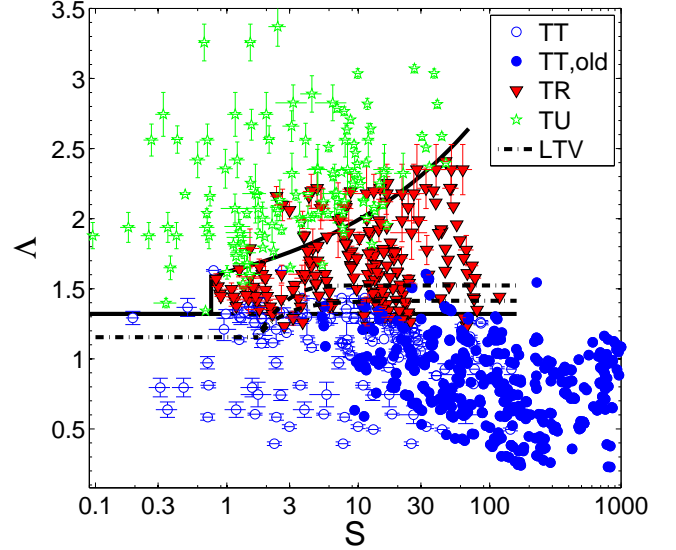

Figure 16. Summary of the motions observed, with coding based on the regime – TU, green stars; TR, red triangles, and TT, blue circles (full symbols - older data[1,2]; empty symbols - newer data[3,4]). Data points are plotted with error bars accounting for the measurement uncertainties. The dash-dotted lines are the dividers given by Lebedev, Turitsyn, and Vergeles[9], while the solid lines are a guide to the eye (for details see text) (color online).

Deschamps *et al.*[4] and obtained from the time series of the vesicle inclination angle, as explained in Section III C. Data from Deschamps, Kantsler, and Steinberg[3] had larger error bars and the regime classification was done by eye; older data[1,2] is only TT (see supplementary

material at [URL will be inserted by AIP] for all data in tabular form). With this caveat and furthermore, with the ambiguities of regime identification of deformed vesicles close to the transition lines, we claim that clustering in different regions is clear. We plot, for reference, the dividers of the regimes given by Lebedev, Turitsyn, and Vergeles[9], respectively $\left\{S < \sqrt{3}, \Lambda = 2/\sqrt{3}\right\}$ for TT/TU, $\left\{S \geq \sqrt{3}, \Lambda = \sqrt{2 - 2/S^2}\right\}$ for TT/TR, and $\left\{S \geq \sqrt{3}, \Lambda = 1.52 - 2.12\, e^{-1.04\, S}\right\}$ for TR/TU (best fit based on the numerical data of their Figure 9).

The extent of the experimental regions deviates from the model. The solid lines in the figure are our eyeball fit to the data, represented by: $\{0 < S < 0.75, \Lambda = 1.32\}$ (TT/TU and TT/TR divider) and $\left\{S > 0.75, \Lambda = 1.32 + 0.3\, S^{0.35}\right\}$ (TR/TU divider). Note the lower Λ transition (to tank treading) has zero slope on both diagrams in the range of our data, for all Δ sampled. The upper line has finite slope for large S, and disagrees with the results of all reduced model simulations. The divider between TR and TU is also less defined on the diagram, in part due to some experimental points with large error bars, but mostly because of ambiguities, namely of vesicles which intermittently flip between large-amplitude trembling and full tumbling rotations, as exemplified by Fig. 11, obtained for $S = 4.7 \pm 0.3$ and $\Lambda = 1.59 \pm 0.03$. A possible explanation for the fact that the upper transition differs greatly from the linear theories and the lower transition does not, is that the former is associated with a saddle-node bifurcation, while the latter with a Hopf type one. It is well known that the nonlinear dynamics associated with the saddle-node transitions are more sensitive to noise than those near Hopf transitions.

The clustering of regimes would be destroyed if the data was plotted, in coordinates $\{\chi, \lambda\}$. In particular, all the experimental data for vesicles with $\lambda = 1$, any regime of motion, would collapse on a single horizontal line. According to Danker et al.[11], Kaoui, Farutin, and Misbah[13], this would happen since the correct dependence on the third parameter, Δ, is not taken into account. However, contrasting this view we plot a subset of our data taken in pure shear flow, in Fig. 17. To compare with Fig. 3 of Farutin, Biben, and Misbah[12], we reproduce their transition curves and select among the available data vesicles with Δ close to the values reported by them. It is rather obvious that the theory[12] disagrees with the data even qualitatively. We do not attempt comparisons between our data in general flow and the Fig. 4 and 5 of Farutin, Biben, and Misbah[12], as not enough data points close to the values displayed there are available.

The dependence on Δ suggested by Noguchi[26] (his Fig. 2a) for vesicles in uniform shear flow is not matched either by the experimental data, as we show in Fig. 18, though the discrepancy is smaller than with the theory of Farutin, Biben, and Misbah[12]. The disagreement between this model, which includes higher order terms, and
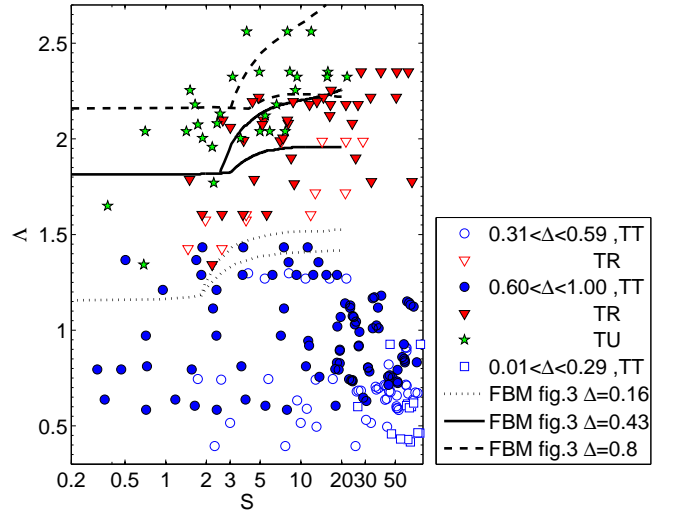

Figure 17. Comparison of our experimental results on the phase diagram with the theory of Farutin, Biben, and Misbah[12] (color online).
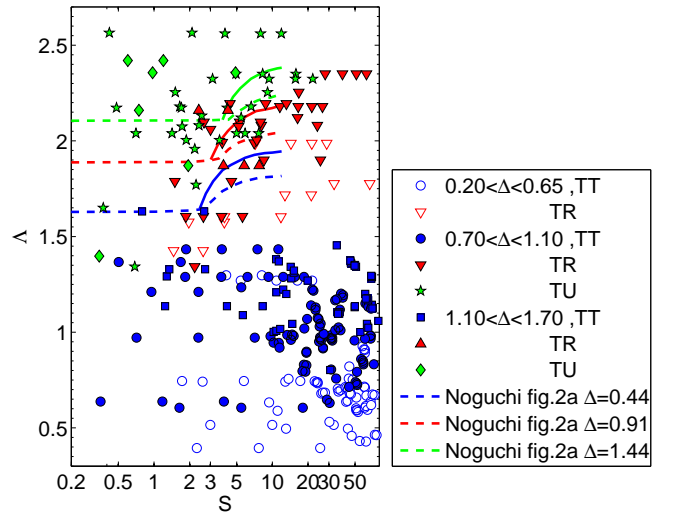

Figure 18. Comparison of our experimental results on the phase diagram with the model of Noguchi[26] (color online).

the phenomenological model of Noguchi[26], is also apparent when comparing Figures 17 and 18.

In summary, we conclude that the coordinates of the LTV phase diagram (Λ vs S) look preferable due to its simplicity, failing the quantitative agreement with data. As we already pointed out[3,4], the LTV theory is based on some assumptions which are not matched by experimental observations. However, puzzling as it may be, the presentation of a two-parameter phase diagram resulting from the self-similar solution of the model provides an adequate description of the data.

V. CONCLUSIONS

In attempt to clarify the mechanisms responsible for vesicle dynamics, we have carefully reexamined existing experimental data, and critically reviewed the recent theoretical and numerical work. We found that despite some qualitative features captured by the existing reduced models, a good quantitative prediction is not achieved. This lack of success may be due to the incomplete understanding and modeling of thermal fluctuations, nonlinear interaction of harmonic modes beyond the second (which can form local regions of negative curvature - which we have seen in the experiments). Present models are derived in the nearly-spherical approximation, and even $\Delta \sim 0.43$ may be considered large. The main conclusion of our analysis is that the agreement between theory and the experimental observations may not improve, not even on a qualitative level, by including in the existing models just some of the necessary elements. In particular, including more even modes without including also odd ones and thermal fluctuations, has been proven unsuccessful either for the description of the TR dynamics or the phase diagram presentation. In any event, we hope that all future modelers will look critically at the effects of noise on transition regimes where $\langle \theta \rangle < 0.15$ radian and where odd modes of vesicle contours are significant.

REFERENCES

[1] V. Kantsler and V. Steinberg, "Orientation and dynamics of a vesicle in tank-treading motion in shear flow," Phys. Rev. Lett. **95**, 258101 (2005).

[2] V. Kantsler and V. Steinberg, "Transition to tumbling and two regimes of tumbling motion of a vesicle in shear flow," Physical Review Letters **96**, 036001 (2006).

[3] J. Deschamps, V. Kantsler, and V. Steinberg, "Phase diagram of single vesicle dynamical states in shear flow," Phys. Rev. Lett. **102**, 118105 (2009).

[4] J. Deschamps, V. Kantsler, E. Segre, and V. Steinberg, "Dynamics of a vesicle in general flow," Proc. Natl. Acad. Sci. U.S.A. **106**, 11444–11447 (2009).

[5] H. Noguchi and G. Gompper, "Fluid vesicles with viscous membranes in shear flow," Phys. Rev. Lett. **93**, 258102 (2004).

[6] H. Noguchi and G. Gompper, "Shape transitions of fluid vesicles and red blood cells in capillary flows," Proc. Natl. Acad. Sci. U.S.A. **102**, 14159 (2005).

[7] H. Noguchi and G. Gompper, "Dynamics of fluid vesicles in shear flow: Effect of membrane viscosity and thermal fluctuations," Physical Review E **72**, 011901 (2005).

[8] S. Messlinger, B. Schmidt, H. Noguchi, and G. Gompper, "Dynamical regimes and hydrodynamic lift of viscous vesicles under shear," Physical Review E **80**, 021902 (2009).

[9] V. V. Lebedev, K. S. Turitsyn, and S. S. Vergeles, "Nearly spherical vesicles in an external flow," New Journal of Physics **10**, 043044 (2008).

[10] V. V. Lebedev, K. S. Turitsyn, and S. S. Vergeles, "Dynamics of nearly spherical vesicles in an external flow," Phys. Rev. Lett. **99**, 218101 (2007).

[11] G. Danker, T. Biben, T. Podgorski, C. Verdier, and C. Misbah, "Dynamics and rheology of a dilute suspension of vesicles: Higher order theory," Physical Review E **76**, 041905 (2007).

[12] A. Farutin, T. Biben, and C. Misbah, "New analytical progress in the theory of vesicles under linear flow," Physical Review E **81**, 061904 (2010).

[13] B. Kaoui, A. Farutin, and C. Misbah, "Vesicles under simple shear flow: Elucidating the role of relevant control parameters," Physical Review E **80**, 061905 (2009).

[14] P. M. Vlahovska, T. Podgorski, and C. Misbah, "Vesicles and red blood cells in flow: From individual dynamics to rheology," Comptes Rendue Physique **10**, 775–789 (2009).

[15] S. Kessler, R. Finken, and R. Seifert, "Elastic capsules in shear flow: Analytical solutions for constant and time-dependent shear rates," European Physical Journal E **29**, 399–413 (2009).

[16] S. Kessler, R. Finken, and R. Seifert, "Swinging and tumbling of elastic capsules in shear flow," J. Fluid Mech. **605**, 207 (2007).

[17] J. M. Skotheim and T. W. Secomb, "Red blood cells and other nonspherical capsules in shear flow: Oscillatory dynamics and the tank-treading-to-tumbling transition," Physical Review Letters **98**, 078301 (2007).

[18] P. Bagchi and R. Kalluri, "Dynamics of nonspherical capsules in shear flow," Physical Review E **80**, 016307 (2009).

[19] S. K. Veerapaneni, D. Gueyffier, D. Zorin, and G. Biros, "A boundary integral method for simulating the dynamics of inextensible vesicles suspended in a viscous fluid in 2d," Journal of Computational Physics **228**, 2334–2353 (2009).

[20] R. Finken, A. Lamura, U. Seifert, and G. Gompper, "Two-dimensional fluctuating vesicles in linear shear flow," European Physical Journal E **25**, 309–321 (2008).

[21] S. K. Veerapaneni, D. Gueyffier, G. Biros, and D. Zorin, "A numerical method for simulating the dynamics of 3d axisymmetric vesicles suspended in viscous flows," Journal of Computational Physics **228**, 7233–7249 (2009).

[22] C. Misbah, "Vacillating breathing and tumbling of vesicles under shear flow," Phys. Rev. Lett. **96**, 028104

(2006).

[23]H. Noguchi and G. Gompper, "Swinging and tumbling of fluid vesicles in shear flow," Phys. Rev. Lett. **98**, 128103 (2007).

[24]H. Noguchi, "Swinging and synchronized rotations of red blood cells in simple shear flow," Physical Review E **80**, 021902 (2009).

[25]U. Seifert, "Fluid membranes in hydrodynamic flow fields: Formalism and an application to fluctuating quasispherical vesicles in shear flow," Eur. Phys. J. B **8**, 405–415 (1999).

[26]H. Noguchi, "Dynamics of fluid vesicles in oscillatory shear flow,"

Journal of the Physical Society of Japan **79**, 024801 (2010).

[27]P. M. Vlahovska and R. S. Gracia, "Dynamics of a viscous vesicle in linear flows," Phys. Rev. E **75**, 016313 (2007).

[28]V. Kantsler, E. Segre, and V. Steinberg, "Vesicle dynamics in time-dependent elongation flow: Wrinkling instability," Phys. Rev. Lett. **99**, 178102 (2007).

[29]K. S. Turitsyn and S. S. Vergeles, "Wrinkling of vesicles during transient dynamics in elongational flow," Phys. Rev. Lett. **100**, 028103 (2008).

[30]U. Seifert, "Configurations of fluid membranes and vesicles," Advances in Physics **46**, 13–137 (1997).